Received: 10 May 2024 | Revised: 29 July 2024 | Accepted: 13 August 2024

DOI: 10.1002/pamm.202400045

RESEARCH ARTICLE

The effect of active leg swing on walking template model dynamics

Daniel Renjewski

Chair of Applied Mechanics, School of Engineering and Design, Technical University of München, Garching, Germany

Correspondence
Daniel Renjewski, Chair of Applied Mechanics, School of Engineering and Design, Technical University of München, Boltzmannstr. 15, 85748 Garching, Germany.
Email: daniel.renjewski@tum.de

Abstract

Some reductionist models match human walking dynamics surprisingly well. For reasons of simplicity, the swing leg and its dynamics have been neglected in the past. A dynamic effect would, however, be expected of the high acceleration and deceleration required to recirculate approximately 15% of the entire body mass during the very short swing phase. This paper documents the investigation of the effect of a simplified swing leg on the dynamics of a reductionist walking model. The findings suggest the dynamic decoupling of the swing leg and the remaining body.

1 | INTRODUCTION

Humans possess a unique mode of locomotion among mammals as the only habitual bipedal *distance* walkers [1], exhibiting remarkable double-humped force patterns during gait [2]. Bipedal movement on two legs introduces intriguing biomechanical challenges involving balance, support, and propulsion. This dynamic interplay necessitates a fascinating reconciliation of two competing objectives: to maximize controllability through prolonged stance phase duration [3, 4], and to efficiently reposition the inert legs within the abbreviated remainder of the gait cycle (GC). The resulting distinctive mechanics invite further exploration of how the human gait has evolved to elegantly address these challenges: the leg in contact with the ground has to provide support and propulsion; the swing leg has to travel a substantial distance in a very short amount of time (Figures 1 and 2) to take over support in the next step.

A step, that is, the duration from the touch-down of one leg to the touch-down of the contra-lateral leg, comprises initial double support and a consecutive single-support phase. Single support, that is, the duration the airborne leg can swing, lasts for an average of 0.35–0.45 s at normal walking speeds.

The following properties characterize bipedal gait:

- **Cycle time (t_c)**: duration from one distinct event of a single leg's action, for example, touch-down, to the next occurrence of the same event at the same leg.
- **Gait frequency (f_c)**: inverse of the cycle time.
- **Duty factor (DF)**: ratio of time a leg spends on the ground to cycle time.

Bipedal walking gaits are composed of consecutive single and double support phases during which one and two legs are in contact with the ground, respectively. Accordingly, the duty factor for walking is well above 0.5, and the remaining time to swing the leg into the next step is comparatively short (Figure 1), even at average walking speeds [5].

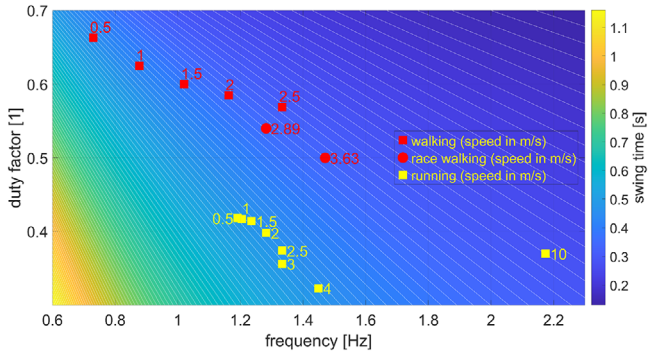

FIGURE 1 Swing time for different human gaits at various velocities. Gait types can be characterized by duty factor while step frequency is more indicative of gait velocity. Walking gaits are characterized by duty factors above 0.5, that is, both legs are sometimes on the ground simultaneously. In contrast, running is characterized by duty factors well below 0.5, indicating phases when no leg touches the ground. White lines indicate constant swing time along each line. Interestingly, absolute swing times are substantially lower for walking than for running, even at higher speeds.

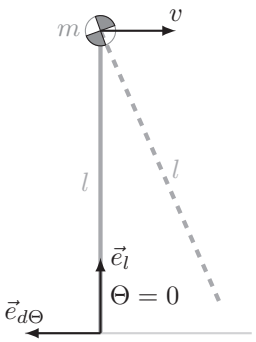

FIGURE 2 The inverted pendulum model at midstance. The parameters are mass (m) and leg length (l), the state is given by Θ and the velocity v as $l\dot{\Theta}$.

1.1 | Reductionist models

The inverted pendulum model (Figure 6), often considered the simplest representation of bipedal walking, can be traced back to the literature as early as 1960 [6]. Over time, it has gained prominence as a foundational model for studying bipedal walking, addressing aspects such as leg swing [7], postural stabilization [8], and the step-to-step transition [9]. Even today, the inverted pendulum model remains a compelling analogy for understanding bipedal walking dynamics [10].

While ref. [7] acknowledged the ballistic nature of leg swing, which often justifies overlooking swing leg dynamics in similar models, the standard approach to generating leg swing in bipedal robots involves applying hip torque. Due to the considerable mass of the leg, it is plausible that this significantly influences gait dynamics.

A shortcoming of the inverted pendulum model is its limitation to model only parts of single support while approximating the double support phase as an instantaneous step-to-step transition. A better approximation of human walking dynamics can be achieved by modeling the leg as a simple, massless spring while keeping the entire mass of the walking body concentrated in a point supported by said spring ([11], Figure 3), which closer resembles the observed dynamics of human bipedal walking [12], referred to as the spring-loaded inverted pendulum model (SLIP).

Both simple models, although capturing parts of the gait dynamics quite accurately, interestingly, do not model a swing leg as the legs are assumed to be massless and thus do not impact the walking dynamics.

1.2 | Humanoid locomotion

Unlike human walking, humanoid robots provide a direct means to study the effects of specific control schemes on gait dynamics. Most humanoid robots utilize hip power to swing their legs, for example, ref. [13], an approach that significantly influences the resulting gait dynamics [14].

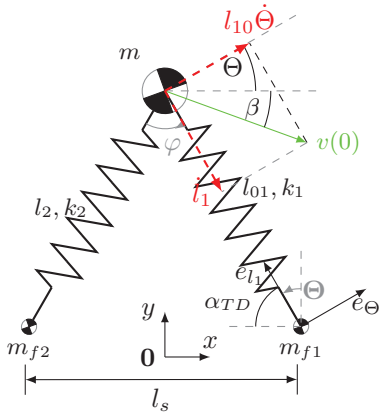

FIGURE 3 Model parameter and coordinates depicted at the instant of touch-down for the SLIP-model [11]. The coordinate system at **0** is spatially fixed, the coordinate system at m_{f1} rotates with Θ. SLIP, spring-loaded inverted pendulum model.

TABLE 1 Parameter definition for the SLIP model (cf. Figure 3), with typical values.

Parameter	Explanation	Typical value	Unit
$l_1(t), l_2(t)$	Current leg (spring) length	0.6–1	m
l_{10}, l_{20}	Resting length of leg springs 1 and 2	1	m
l_s	Step length	0.5–1	m
k_1, k_2	Stiffness of leg springs 1 and 2	10–30	kN
m	Overall mass	80	kg
m_f	Mass of a foot/leg	11% m	kg
α_{TD}	Leg angle at touch-down (angle of attack)	65–80	o
$\beta(t)$ velocity angle w.r.t. +x	−45–45	o	

In this work, I delve into this influence by incorporating a swinging leg into the simplest walking model, seeking to uncover and understand its effects on overall gait dynamics. It is hypothesized that swinging the leg actively during the swing phase through hip actuation will result in noticable dynamics changes of resulting global dynamics compared to normal human walking dynamics.

2 | MODELING

The common bipedal SLIP model comprises a single mass point connected through springs to a rigid ground. It models bipedal locomotion in the sagittal plane and has two degrees of freedom ([11], Figure 3, Table 1). The typical motion of the model, in agreement with normal human walking, is divided into single and double support phases. Phase transitions are marked by take-off and touch-down events of each leg in succession. During single support following take-off, the leg that has just lost contact with the ground swings forward, ending the single support phase by touching down again.

I extend the SLIP model to feature leg masses representing the common mass distribution in humans and robots [15]. The distributed masses have no effect in double-support as both foot masses are stationary on the ground. A generalized force will be added to the Lagrange equation during single support and two independent degrees of freedom for the swing leg ($[\ddot{x}_f, \ddot{y}_f]$). I assume that during single support, the spring of the swing leg is inactive and refer to this extended model as *swSLIP*. The following parameters are defined for the model.

2.1 | Model state

The motion of the model, commonly expressed in cartesian coordinates when no swing leg is considered, is described in polar coordinates Θ and l (Figure 3) as it appears to simplify the mathematical description of the swing leg. The polar

coordinate system is placed at the position of the foot that touched down last and is thus shifted from one foot to the other at each touch-down with the required coordinate transformation. The vector of the generalized coordinates $\vec{q}$ and its derivative are introduced (Equations 1 and 2). The position of the model's main mass (m) can thus be expressed in generalized coordinates (Equation 3).

$$\vec{q}(t) = \begin{pmatrix} \Theta(t) \\ l_1(t) \end{pmatrix} \tag{1}$$

$$\dot{\vec{q}} = \begin{pmatrix} \dot{l}_1 \\ \dot{\Theta}_1 \end{pmatrix} \tag{2}$$

$$\vec{r}_{hip}(q) = \begin{pmatrix} -l_1(t)sin(\Theta(t)) \\ l_1(t)cos(\Theta(t)) \end{pmatrix} \tag{3}$$

2.2 | Phasing and initial conditions

Events at specific points of the GC couple the phases of the hybrid dynamical model. The simulation will start at the beginning of a double support phase, with leg 1 being considered the leg touching down in this instant. At that point, I assume that $\Theta \Longleftarrow \alpha_{TD}$, the length of the leg touching down is equal to the spring's resting length l_{01}, and thus, along with the step length l_S, determines the state of the model. Thus the initial conditions are determined as

$$\begin{aligned} l_1(0) &= l_{10} \\ \Theta(0) &= \pi/2 - \alpha_{TD} \end{aligned} \tag{4}$$

Also, the time derivatives of the boundary conditions are required and have to be derived from the initial Center of mass (CoM) velocity.

I can formulate the derivatives by projecting v onto the leg and the perpendicular to the leg (Figure 3) as

$$\begin{aligned} \dot{l}_1(0) &= -v(0)\sin(\beta(0) + \Theta(0)) \\ \dot{\Theta}(0) &= \frac{v(0)\cos(\beta(0) + \Theta(0))}{l_{10}}. \end{aligned} \tag{5}$$

Thus, the vector of initial conditions consists of $S_0 = [v, \beta, l_{10}, \alpha_{TD}, l_S]$ from which all other initial states can be derived.

2.3 | Swing leg dynamics

The motion of the swing leg is described in cartesian coordinates by $\vec{r}_f = [x_f\ y_f]^T$. Accordingly, the dynamic reaction at the "hip" joint during the swing phase is described in Cartesian coordinates. I model the swing leg as an excited pendulum with two degrees of freedom, where the driving force actively influences both, represented by $\ddot{\vec{r}}_f$ with gravity (g) factored into $\ddot{\vec{r}}_{f,y}$ (Figures 4 and 5). I can write the equations of motion for the swing leg in vector components as

$$\begin{aligned} x &: m_{f2}\ddot{r}_{f,x} = G_x \\ y &: m_{f2}\ddot{r}_{f,y} = G_y \\ M_z^{(hip)} &: m_{f2}l^2\ddot{\gamma}_z = m(\vec{r}_{hip} - \vec{r}_f) \times \ddot{\vec{r}}_f = M_{G,z} \end{aligned} \tag{6}$$

While the forces can be easily expressed in cartesian coordinates, an explicit expression for the torque dependent on γ requires a projection onto a leg coordinate system which originates at the hip and is rotated w.r.t. the cartesian coordinates

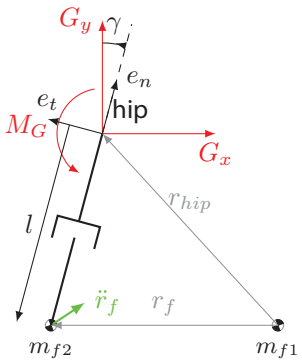

FIGURE 4 Swing leg dynamics and parameters. The swing leg has two degrees of freedom ($[\gamma, l]$). The resulting internal forces can be determined by a swing leg acceleration $\ddot{r}_f$. The position of hip and swing foot (m_{f2}) is given by the depicted vectors which originate at the coordinate system m_{f1}.

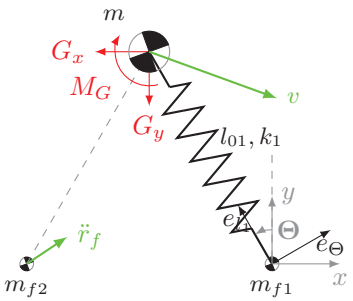

FIGURE 5 The SLIP model during the stance phase with the internal forces/torque resulting from leg swing indicated. In addition, gravity and spring force are acting on m. Section 2.4.1 describes the projection of the internal forces onto the generalized coordinates. SLIP, spring-loaded inverted pendulum model.

by γ (Figure 4).

$$A(\gamma) = \begin{pmatrix} \cos\gamma & -\sin\gamma & 0 \\ \sin\gamma & \cos\gamma & 0 \\ 0 & 0 & 1 \end{pmatrix} \tag{7}$$

By rotating the forces at the pivot, the tangential force component F_t, perpendicular to l, can be determined as

$$\begin{pmatrix} F_t \\ F_n \end{pmatrix} = A(\gamma)\begin{pmatrix} G_x \\ G_y \end{pmatrix} = A(\gamma) m_{f2} \ddot{\vec{r}}_f. \tag{8}$$

Thus, equation of motion for the tangential component in polar coordinates

$$m_{f2}(2\dot{l}\dot{\gamma} + l\ddot{\gamma}) = F_t, \tag{9}$$

yields an expression for $\ddot{\gamma}$ as

$$\ddot{\gamma} = \frac{\frac{F_t}{m_{f2}} - 2\dot{l}\dot{\gamma}}{l}, \tag{10}$$

which in turn can be used to determine the resulting torque M_z^{hip} as

$$\begin{aligned} M_z^{hip}(\ddot{r}_f, \dot{\gamma}, \dot{l}) &= m_{f2} l^2 \ddot{\gamma} = m_{f2} l \left(\frac{F_t}{m_{f2}} - 2\dot{l}\dot{\gamma}\right) = (F_t - 2m_{f2}\dot{l}\dot{\gamma})l \\ &= \left[\cos\gamma \ddot{r}_{f,x} + \sin\gamma \ddot{r}_{f,y} - 2\dot{l}\dot{\gamma}\right] m_{f2} l. \end{aligned} \tag{11}$$

Thus, at the pivot (hip), the acting torque and forces can be formulated in cartesian coordinates as

$$\vec{F}(\ddot{r}_f) = m_{f2}\ddot{\vec{r}}_f; \quad \vec{M}(\ddot{r}_f, \dot{\gamma}, \dot{l}) = m_{f2} l \begin{pmatrix} 0 \\ 0 \\ \cos\gamma \ddot{r}_{f,x} + \sin\gamma \ddot{r}_{f,y} - 2\dot{l}\dot{\gamma} \end{pmatrix}. \tag{12}$$

2.4 | Swing/stance leg synchronization

I base the model of leg swing on the following assumptions: (1) the leg needs to be accelerated and decelerated to achieve the required displacement and touch down softly, (2) sufficient ground clearance during swing needs to be ensured to prevent foot scuffing or stumbling, (3) swing has to be completed in the time it takes the rest of the body to complete its single support phase and reach a state suitable for touch-down. During swing, I assume the foot mass to be completely free to move.

I define τ as a normalized swing time. The parameter swing time (t_s), which results from model dynamics is introduced. The normalized time during a swing is defined as

$$\tau(t) = \left(\frac{(t - t_{s0})}{t_s} - 0.5\right) \cdot 2\pi \mid \tau \epsilon [-\pi, \pi], \tag{13}$$

with t_{s0} being the take-off time of the leg transitioning into swing. Now, I formulate the desired, parameterized accelerations for the swing leg as a smooth function to meet the requirements listed above:

$$\ddot{\vec{r}}_f = \begin{pmatrix} \ddot{x}_{fs} \\ \ddot{y}_{fs} \\ 0 \end{pmatrix} = \begin{pmatrix} -\sin(\tau) \cdot a_x \\ -a_y \cdot \text{sign}\,(x + a_{y2}) + a_{ay3} \\ 0 \end{pmatrix}. \tag{14}$$

Note that this is an arbitrary choice and other functions, for example, a step function, would be possible.

2.4.1 | Projection onto generalized coordinates

To project force and torque onto the generalized coordinates I determine the respective velocities $\dot{\vec{r}}$ and $\vec{\omega}$ with $|\vec{\omega}| = \dot{\Theta}$ describing the rotation of the system around the z-axis pointing towards the reader. The respective vectors are

$$\dot{\vec{r}}_{hip} = \begin{bmatrix} -\dot{l}_1(t)\sin(\Theta(t)) - l_1(t)\cos(\Theta(t))\dot{\Theta}(t) \\ \dot{l}_1(t)\cos(\Theta(t)) - l_1(t)\sin(\Theta(t))\dot{\Theta}(t) \\ 0 \end{bmatrix} = A\left(\frac{\pi}{2} + \Theta\right) \begin{pmatrix} \dot{l}_1 \\ l_1\dot{\Theta} \\ 0 \end{pmatrix}, \quad \text{and} \tag{15}$$

$$\vec{\omega} = \begin{pmatrix} 0 \\ 0 \\ \dot{\Theta} \end{pmatrix}, \tag{16}$$

which can be projected with the following Jacobi-Matrices:

$$\mathbf{J}_r = \frac{\delta \dot{\vec{r}}_{hip}}{\delta \dot{\vec{q}}} = \begin{pmatrix} -\cos(\Theta(t))l_1(t) & -\sin(\Theta(t))l_1(t) & 0 \\ -\sin(\Theta(t)) & \cos(\Theta(t)) & 0 \end{pmatrix}, \text{ and} \tag{17}$$

$$\mathbf{J}_M = \frac{\delta \vec{\omega}}{\delta \dot{\vec{q}}} = \begin{pmatrix} 0 & 0 & 1 \\ 0 & 0 & 0 \end{pmatrix}, \tag{18}$$

that are obtained by calculating the derivative of $\dot{\vec{r}}_{hip}$ (Equation 15) and $\vec{\omega}$ (Equation 16) w.r.t. $\dot{\vec{q}}$ (Equation 2). Accordingly, the generalized force projected from cartesian onto generalized coordinates will be

$$\vec{Q} = \mathbf{J}_r \vec{F}_s + \mathbf{J}_M \vec{M}_G. \tag{19}$$

Thus, I can now derive the equations of motion from

$$\frac{d}{dt}\left(\frac{\partial L}{\partial \dot{\vec{q}}}\right) - \frac{\partial L}{\partial \vec{q}} = \vec{Q}, \tag{20}$$

for which I only write the scalar components $\nabla L(q)$ for each component of $\vec{q}$.

2.5 | Cyclic gait and optimization

Walking is a cyclic motion that leaves the walker close to its initial state after a completed step for all cyclic states. The GC starts at the beginning of double support with touch down. The initial conditions are described in Section 2.2. Along with the initial conditions, the parameters for the swing leg dynamics, namely $[t_s, a_x, a_y, a_{y2}]$, must be passed to the optimizer. I want to optimize the parameters such that

① The swing leg is fully extended at touch-down and lands on the ground

$$\begin{aligned} l_{TD} &= |[x, y]^T - [-l_s \sin(\Theta), l_s \cos(\Theta)]^T| \\ \mathcal{O}(①) &= |l_{TD} - l_{20}|; \end{aligned} \tag{21}$$

② It touches down with the predetermined touch-down angle

$$\begin{aligned} \alpha_l &= \arctan \frac{l_1 cos(\Theta) - y_f}{x_f - l_1 sin(\Theta)} \\ \mathcal{O}(②) &= |\alpha_l - \alpha_{TD}|; \end{aligned} \tag{22}$$

③ The point of touch-down is one predetermined step length away from the stance leg

$$\mathcal{O}(③) = x(end) - l_s; \tag{23}$$

④ The velocity at touch-down matches the initial velocity

$$\begin{aligned} \dot{\vec{r}}_0 &= [-\dot{l}_{10} \sin \Theta_0 - l_{10} \cos \Theta_0 \dot{\Theta}_0, \dot{l}_{10} \sin \Theta_0 - l_{10} \sin \Theta_0 \dot{\Theta}_0]^T \\ \dot{\vec{r}}_e &= [-\dot{l}_{1e} \sin \Theta_e - l_{1e} \cos \Theta_e \dot{\Theta}_e, \dot{l}_1 e \sin \Theta_e - l_{1e} \sin \Theta_e \dot{\Theta}_e]^T \\ \mathcal{O}(④) &= ||\dot{\vec{r}}_e - \dot{\vec{r}}_0||; \end{aligned} \tag{24}$$

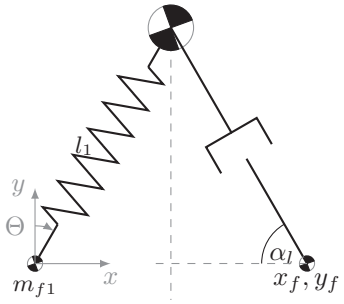

FIGURE 6 Model configuration before touch-down. The current angle of attack α_l is determined from the position of the swing foot ($[x_f, y_f]^T$) and the position of the main mass as expressed in Equation (22).

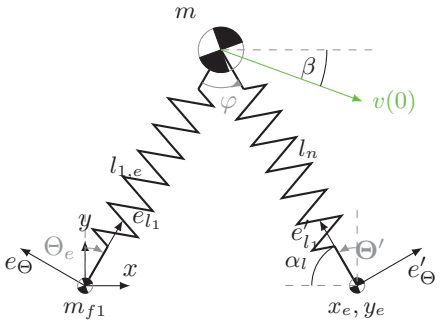

FIGURE 7 The model after touch-down. In preparation for the take-off of the trailing leg m_{f1}, the coordinate system has to be shifted from m_{f1} to m_{f2} and the model states transformed. Given the final length of the trailing leg ($l_{1,e}$) and the terminal leg angle $\Theta - e$, the inter-leg angle φ can be used to transform all states to the new coordinate system.

⑤ The velocity of the foot ensures maximum ground speed matching

$$\mathcal{O}(⑤) = |y|. \tag{25}$$

The objective function can be formulated as

$$O = \sum_{i=1}^{5} \mathcal{O} \tag{26}$$

2.6 | Transition to the second double support

After completing the single support phase, a transition into the subsequent double support phase is required. As the current stance leg will soon transition into swing, a coordinate transformation is necessary, shifting the coordinate system from the now trailing leg to the newly touched down leg (Figure 7). Note, that the length of the leg that just touched down is not necessarily exactly the spring's resting leg, subject to the optimization result. Therefore, new initial conditions $[\Theta' \; l_n \; \dot{\Theta}' \; \dot{l}_n]^T$ need to be calculated as follows:

$$\begin{aligned}
l_n &= |[x_e, 0]^T - \vec{r}_{hip}| \\
\Theta' &= \pi/2 - \arcsin\left(\frac{l_{1e}\sin(\pi/2 - \Theta_e)}{\sqrt{l_{1e}^2 + x_e^2 - 2l_{1e}x_e\cos(\pi/2 - \Theta_e)}}\right), \\
\begin{pmatrix} \dot{l}_{1n} \\ \dot{\Theta}' l_n \end{pmatrix} &= \begin{pmatrix} \cos(-\varphi) & -\sin(-\varphi) \\ \sin(-\varphi) & \cos(-\varphi) \end{pmatrix} \begin{pmatrix} \dot{l}_{1e} \\ \dot{\Theta}_e l_{1e} \end{pmatrix},
\end{aligned} \tag{27}$$

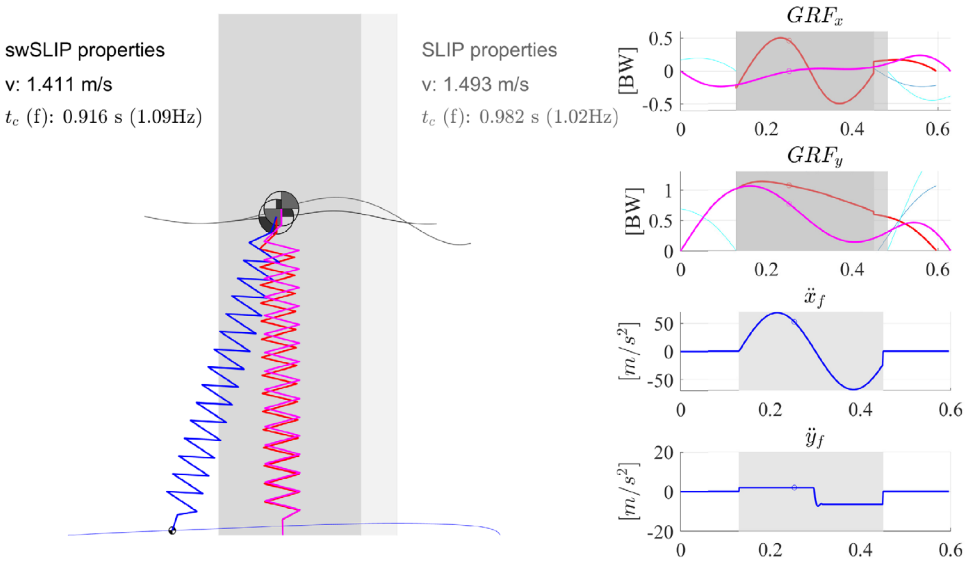

FIGURE 8 CoM trajectories of swSLIP (red/black CoM) and SLIP (magenta/gray CoM) model with identical initial conditions. Both models are shown at about midstance. Vertical and horizontal ground reaction force as well as the required swing leg acceleration for the swSLIP's swing leg (blue) are shown. Single support phases are indicated by dark gray (swSLIP) and light gray (SLIP). CoM, center of mass; SLIP, spring-loaded inverted pendulum model.

with φ calculated as

$$\varphi = \arcsin \frac{l_{1e} \sin(\pi/2 - \Theta_e)}{\sqrt{l_{1e}^2 + x_e^2 - 2 l_{1e} x_e \cos(\pi/2 - \Theta_e)}}. \tag{28}$$

3 | RESULTS

The optimized parameters as well as the resulting dynamics are reported in this section.

3.1 | Optimization results

Initial states to start the optimization are set to

Parameter	v_0 [m/s]	β [rad]	α_{TD} [deg]	l_s [m]	t_s [s]	a_x [m/s²]	a_y [m/s²]	a_{y2} [m/s²]	a_{y3} [m/s²]
Value	1.5	$-\pi/16$	75 °	0.54	0.3	55	7	0	9.81
Limits	[1.45, 1.7]	$[-\pi/8, -\pi/20]$	[65 °, 80 °]	[0.6,1]	[0.15,0.45]	[1,70]	[4, 50]	$[-\pi, \pi]$	[0,20]
Result I	1.64	–0.18	66.5	0.62	0.34	68.3	4.23	0	7.48

3.2 | Simulation results

The optimizer (*fmincon*, MATLAB 2024a, The Mathworks, Natick, USA) found a solution for a sufficiently cyclic motion for the swSLIP model (Figure 8). A common SLIP model has been modeled with identical initial conditions for comparison. The resulting ground reaction forces (GRF) for any leg in stance during a given period and the resulting swing leg accelerations are shown. Both models show normal average walking speeds and fairly realistic cycle times (comp. Figure 1). The initial conditions found for the swSLIP model do unsurprisingly not lead to a periodic gait for the SLIP

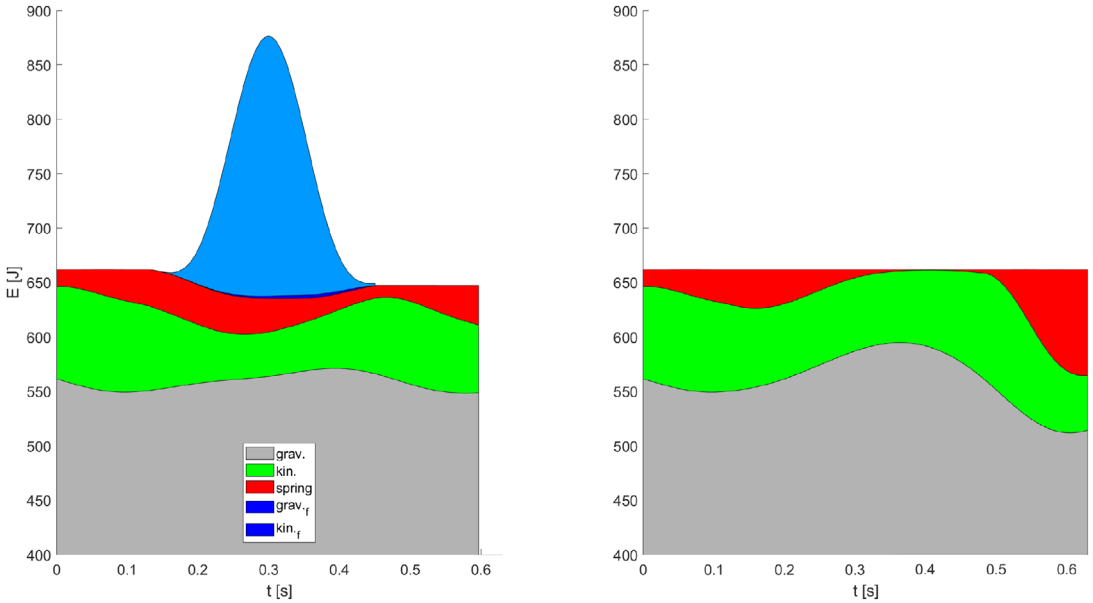

FIGURE 9 Mechanical energy contribution for the swing leg model (left) and classic spring-mass model for walking (right).

model. The comparison, however, makes it apparent that the vertical oscillation in the swSLIP model and the velocity during single support and the single support duration are reduced due to the swing leg dynamics.

Most importantly, the high horizontal accelerations of the swing leg ($\ddot{x}_f$) substantially modify the horizontal ground reaction forces (GFR_x) in comparison to those observed in human (Figure 8, top left.). However, GRF observed in walking experiments with the humanoid robot Lola that drives leg swing from the hip exhibit a similar inversion in horizontal GRF [14, Figure 4c], while human subjects aiming to imitate the gait of the robot retain their normal walking force profile.

The required peak accelerations of more than 50 m/s^2 for leg recirculation in the given amount of time (here 0.32 s for the swSLIP model and 0.35 s for the SLIP model) lead to clearly modified global dynamics (Figure 8, right panel). In contrast to the traditional spring-mass model, adding a swing leg renders the model energy non-conservative. Mechanical energy is added to facilitate leg swing and dissipated at touch-down (Figure 9). Gravitational and elastic potential energy, as well as kinetic energy of the model's CoM and the swinging leg, have been accounted for when considering the swSLIP model. Again, the leg swing adds substantially to the total model energy due to the leg's kinetic contribution. The difference in total energy between the initial and terminal double support phases is caused by a non-perfect touch-down state, that is, at the end of the swing, the "foot" is not exactly at ground level and exhibits a velocity mismatch.

4 | DISCUSSION

The swSLIP model suggests an explanation for the GRFs observed in the motion of our robot, which drives leg swing from the hip. Discrepancies in human walking indicate a decoupled swing leg powered from a different source. The ankle catapult [16, 17] is a promising candidate to drive ballistic walking as proposed by Mohon [7], providing a functional explanation for the large power output observed in human walking.

The presented result is, however, not conclusive as the trunk could serve as a dynamic counterweight for swing leg dynamics. In a future study, the proposed model will be extended to feature a rigid trunk with physiologically plausible inertia and investigate how this can mitigate the swing leg's effect on global gait dynamics. Given the small overall excursions of the trunk, the amount of counter torque could be limited, still requiring another power source for swinging the leg. This is strongly supported by the matching dynamics of reductionist models with massless legs.

Given the mass of the foot on a long lever (leg), the torque/velocity (power) requirements for swing actuation from the hip are large. This limits the pacing of phase sequencing for bipedal robots and, therefore, their maximum speed, leading to inefficient gaits and overpowered actuators.

5 | CONCLUSION

Our findings suggest that models with massless legs accidentally provided a good approximation for the impact of leg swing on global gait dynamics. The underlying function of leg swing has the potential to lead to more efficient and adaptable walking humanoid robots.

ACKNOWLEDGMENTS

Open access funding enabled and organized by Projekt DEAL.

ORCID

Daniel Renjewski https://orcid.org/0000-0001-9615-2241

REFERENCES

1. Klenerman, L., & Wood, B. (2006). *The human foot*. Springer. https://link.springer.com/book/10.1007/b136908
2. Alexander, R. M. (2004). Bipedal animals, and their differences from humans. *Journal of Anatomy*, *204*(5), 321–330. https://doi.org/10.1111/j.0021-8782.2004.00289.x
3. Lee, C. R., & Farley, C. T. (1998). Determinants of the center of mass trajectory in human walking and running. *Journal of Experimental Biology*, *201*(Pt), 21. https://doi.org/10.1242/jeb.201.21.2935
4. Cairns, M. A., Burdett, R. G., Pisciotta, J. C., & Simon, S. R. (1986). A biomechanical analysis of racewalking gait. *Medicine & Science in Sports & Exercise*, *18*(4), 446–453. https://www.ncbi.nlm.nih.gov/pubmed/3747807
5. Bornstein, M. H., & Bornstein, H. G. (1976). The pace of life. *Nature*, *259*(5544), 557–559. https://doi.org/10.1038/259557a0
6. Cotes, J. E., & Meade, F. (1960). The energy expenditure and mechanical energy demand in walking. *Ergonomics*, *3*(2), 97–119. https://doi.org/10.1080/00140136008930473
7. Mochon, S., & McMahon, T. A. (1980). Ballistic walking. *Journal of Biomechanics*, *13*(1), 49–57. https://doi.org/10.1016/0021-9290(80)90007-x
8. Chow, C. K., & Jacobson, D. H. (1972). Further studies of human locomotion: Postural stability and control. *Mathematical Biosciences*, *15*(1-2), 93–108. https://doi.org/10.1016/0025-5564(72)90065-x
9. Kuo, A. D. (2002). Energetics of actively powered locomotion using the simplest walking model. *Journal of Biomechanical Engineering*, *124*(1), 113–120. https://doi.org/10.1115/1.1427703
10. Holowka, N. B., & Lieberman, D. E. (2018). Rethinking the evolution of the human foot: Insights from experimental research. *The Journal of Experimental Biology*, *221*(17). https://doi.org/10.1242/jeb.174425
11. Geyer, H., Seyfarth, A., & Blickhan, R. (2006). Compliant leg behaviour explains basic dynamics of walking and running. *Proceedings of the Royal Society B: Biological Sciences*, *273*(1603), 2861–2867. https://doi.org/10.1098/rspb.2006.3637
12. Lipfert, S. W., Günther, M., Renjewski, D., Grimmer, S., & Seyfarth, A. (2012). A model-experiment comparison of system dynamics for human walking and running. *Journal of Theoretical Biology*, *292*, 11–17. https://doi.org/10.1016/j.jtbi.2011.09.021
13. Seiwald, P., Sygulla, F., Staufenberg, N. S., & Rixen, D. (2019). Quintic spline collocation for real-time biped walking-pattern generation with variable torso height. *International Conference on Humanoid Robots (Humanoids)* (pp. 56–63). IEEE. https://doi.org/10.1109/humanoids43949.2019.9035076
14. Vielemeyer, J., Staufenberg, N. S., Schreff, L., Rixen, D., & Müller, R. (2023). Walking like a robot: Do the ground reaction forces still intersect near one point when humans imitate a humanoid robot? *Royal Society Open Science*, *10*(5). https://doi.org/10.1098/rsos.221473
15. Wittmann, R. (2012). *Online Gangmusterplanung für humanoide Roboter*. Diplomathesis. https://mediatum.ub.tum.de/1135361
16. Lipfert, S. W., Günther, M., Renjewski, D., & Seyfarth, A. (2014). Impulsive ankle push-off powers leg swing in human walking. *Journal of Experimental Biology*, *217*(Pt 8), 1218–1228. https://doi.org/10.1242/jeb.097345
17. Renjewski, D., Lipfert, S., & Günther, M. (2022). Foot function enabled by human walking dynamics. *Physical Review E*, *106*(6), 064405. https://doi.org/10.1103/PhysRevE.106.064405

How to cite this article: Renjewski, D. (2024). The effect of active leg swing on walking template model dynamics. *Proceedings in Applied Mathematics and Mechanics*, *24*, e202400045. https://doi.org/10.1002/pamm.202400045